Electronic Supplementary Material (ESI) for Journal of Materials Chemistry A.
This journal is © The Royal Society of Chemistry 2024

Supporting information

Two New Cd-based Metal-organic Frameworks for Afterglow Detection of Fe^{3+} and NH_3

Wen-Qi Zhang,[a] *Bo-Lun Zhang,*[b] *Ting Wang,*[a] *Jun Chen,*[b] *Zhong-Yi Li,* [*c] *Rui-Hong Wang,*[a]

Shuqin Liu[b] *and Jian-Jun Zhang*[*a]

[a] School of Chemistry, Dalian University of Technology, Dalian 116024, China. E-mail:

zhangjj@dlut.edu.cn

[b] School of Chemical Engineering, Dalian University of Technology, Dalian 116024, China.

[c] College of Chemistry and Chemical Engineering, Shangqiu Normal University, Shangqiu

476000, China. E-mail: lizhyi84@163.com

Experimental Procedures

1. Materials and measurements

All commercially available reagents and solvents were used as received without further purification. Thermogravimetric analyses (TGA) were performed under N_2 atmosphere with a heating rate of 10°C/min using a TA-Q50 thermogravimetric analyzer. Powder X-ray diffraction pattern (PXRD) data were collected on the Rigaku SmartLab 9KW diffractometer. The infrared spectra within the range of 4000 ~ 400 cm^{-1} were recorded on the Nicolet 6700 spectrometer. The UV visible absorption spectra were collected on the Lambda 750S UV visible spectrophotometer. The luminescence spectrum at room temperature were obtained on a Hitachi F-7000 fluorescence spectrophotometer, in which the chopping speed was selected as 40 Hz for the delayed emission spectra test. The luminescence lifetime of the samples were recorded on on an Edinburgh Instruments FLS1000 spectrophotometer (Instrumental Analysis Center of DUT). Photoluminescence graphs were taken using a smartphone (iPhone 13) under UV lamp irradiation. H_2L was synthesized according to the reported literature.[1]

Synthesis of $[Cd(L)(DMSO)_2]$ (1)

A mixture containing 24.7 mg of $Cd(NO_3)_2 \cdot 4H_2O$ (0.08 mmol), 12.3 mg of H_2L (0.04 mmol) in DMSO/DMF/EtOH/H_2O (1.5 ml/1 mL/0.5 mL/0.5 mL) in a 20 mL scintillation vial was heated at 85°C for 24 hours and then cooled to room temperature. The colorless needle crystals were collected, washed with DMSO and dried in air (63% yield based on ligand). Element analysis (%) calcd for $C_{20}H_{19}CdN_3O_6S_2$: C, 41.85; H, 3.34; N, 7.32. Found: C, 41.83; H, 3.37; N, 7.36. IR (cm^{-1}): 3108 (w), 3010 (w), 3042 (w), 2914 (w), 1765 (m), 1109 (m), 1590 (s), 1540 (s), 845 (s), 1376 (s), 1700 (vs).

Synthesis of $[CdL(H_2O)(DMF)_{0.5}(DMSO)_{0.5}] \cdot DMF$ (2)

A mixture containing 21.3 mg of $Cd(CH_3COO)_2 \cdot 2H_2O$ (0.08 mmol), 12.3 mg of H_2L (0.04 mmol) in DMSO/DMF/H_2O (0.5 ml/3 mL/0.8 mL) in a 20 mL scintillation vial was heated at 85°C for 24 hours and then cooled to room temperature. The colorless crystals were collected, washed with DMF and dried in air (75% yield based on ligand). Element analysis (%) calcd for $C_{21.5}H_{22.5}CdN_{4.5}O_7S_{0.5}$: C, 44.19; H, 3.88; N, 10.78. Found: C, 44.22; H, 3.85; N, 10.82. IR (cm^{-1}): 3300 (w), 1764 (m), 1600 (m), 1400 (s), 846 (s), 782 (s), 1545 (s), 1373 (vs), 1312 (vs), 1008 (vs), 1705 (vs).

X-ray Crystallographic Study

Intensity data of single crystals was measured on a Bruker SMART APEX II CCD area detector system. Data were corrected for absorption effects using the multi-scan technique (SADABS). The structure was

solved by direct methods using SHELXS-2014 and was refined by full-matrix least squares methods using SHELXS-2014.[2] All nonhydrogen atoms were refined anistropically. The hydrogen atoms were included in the structural model as fixed atoms "riding" on their respective carbon atoms using the idealized sp^2-hybridized geometry and C–H bond lengths of 0.95 Å. A summary of the most important crystal and structure refinement data is given in **Table S1**. Selected bond distances and angles are given in **Table S2** and **S3**. CCDC 2321760-2321761 contain the supplementary crystallographic data for this paper. The data can be obtained free of charge via www.ccdc.cam.ac.uk/conts/retrieving.html (or from the Cambridge Crystallographic Data Centre, 12 Union Road, Cambridge CB2 1EZ, UK; fax: (+44) 1223-336-033; or e-mail: deposit@ccdc.cam.ac.uk).

Luminescence sensing of ions in dispersions

Each sensing experiment was repeated at least three times with consistent results. 5 mg finely-ground powder of **1** (or **2)** was dispersed in 10 mL EtOH (DMAc for **2**), ultrasonicated for 20 min to form a stable emulsion for luminescence experiment. An EtOH solution of M^{x+} (0.1 M) was prepared at room temperature for the detection experiment of **1** (M^{x+} = Ni^{2+}, Zn^{2+}, Cd^{2+}, Co^{2+}, Mn^{2+}, Mg^{2+}, Cu^{2+}, K^{+}, Li^{+}, Na^{+}, Ca^{2+}, Al^{3+}, Cr^{3+}, Pb^{2+}, Fe^{3+}). In the luminescence titration experiment, Fe^{3+} solutions were added into the suspension, then the delayed emission spectra were recorded under 365 nm excitation. The excitation slit width and emission slit width in luminescent measurements were set to be 10 nm and 10 nm, respectively.

In the amines/NH_3 sensing experiment, DMAc solutions of amines/NH_3 were added into the suspension, then the delayed emission spectra were recorded under 365 nm excitation. In the solid vapor sensing experiment, different amounts of NH_3•H_2O vapor was saturated in a closed container at 30°C, and then the grooved quartz sheets containing 8 mg samples were placed in each environment for vapor response. After ~ 35 mins, the delayed emission spectrum was recorded under 365 nm UV excitation. The excitation slit width and emission slit width were set to be 10 nm and 10 nm, respectively.

2. Tables

Table S1. Crystallographic data for compounds **1** and **2**.

Formula	$C_{20}H_{19}CdN_3O_6S_2$	$C_{21.50}H_{22.50}CdN_{4.50}O_7S_{0.50}$
Formula weight	573.90	584.37
Crystal system	Orthorhombic	Monoclinic
Space group	*Pbca*	*C2/c*
a (Å)	15.9088(6)	25.033(3)
b (Å)	9.5047(3)	16.8091(17)
c (Å)	29.4059(11)	11.8586(12)
α(°)	90	90
β(°)	90	97.545(4)
γ(°)	90	90
V ($Å^3$)/Z	4446.4(3)/8	4946.7(9)/8
D_{calcd} (g /cm^3)	1.715	1.569
F(000)	2304	2360
θ range(°)	2.561 ~ 24.998	1.463 ~ 24.996
Reflections collected/unique	38273/5099	30405/4345
R(int)	0.0608	0.0457
GOF on F^2	1.144	1.018
limiting indices	-14≤ h ≤ 18	-29≤ h ≤29
	-11≤ k ≤ 11	-19≤ k ≤ 19
	-34≤ l ≤ 34	-14≤ l ≤ 14
R_1, I>2σ(I) (all)	0.0282(0.0605)	0.0321(0.0361)
wR_2 , I>2σ(I) (all)	0.0407(0.0648)	0.0830(0.0853)

*R= ∑(||F_o|-|F_c||) / ∑ |F_o| , **wR = {∑w [(F^2_o – F^2_c)] / ∑w [(F^2_o) ^{2}]}$^{0.5}$, w = [σ^2(F^2_o) + (aP)^2+bP] $^{-1}$, where P = (F^2_o +2F^2_c)/3. For **1**, a = 0.0236, b = 8.3680. For **2**, a = 0.0446， b = 18.5808.

Table S2. Selected bond lengths (Å) and angles (°) for **1**.

Cd(1)-O(5)	2.230(2)	N(1)#2-Cd(1)-O(4)	94.56(8)
Cd(1)-N(2)#1	2.247(2)	O(5)-Cd(1)-O(6)	79.52(9)
Cd(1)-N(1)#2	2.248(3)	N(2)#1-Cd(1)-O(6)	100.98(9)
Cd(1)-O(4)	2.330(2)	N(1)#2-Cd(1)-O(6)	86.51(9)
Cd(1)-O(6)	2.377(2)	O(4)-Cd(1)-O(6)	119.53(8)
Cd(1)-O(3)	2.464(2)	O(5)-Cd(1)-O(3)	100.52(8)
O(5)-Cd(1)-N(2)#1	92.06(9)	N(2)#1-Cd(1)-O(3)	84.72(8)
O(5)-Cd(1)-N(1)#2	164.69(9)	N(1)#2-Cd(1)-O(3)	92.75(8)
N(2)#1-Cd(1)-N(1)#2	96.76(9)	O(4)-Cd(1)-O(3)	54.87(7)
O(5)-Cd(1)-O(4)	86.98(8)	O(6)-Cd(1)-O(3)	174.30(8)
N(2)#1-Cd(1)-O(4)	138.46(8)		

Symmetry transformations used to generate equivalent atoms in 1:

#1 x,-y+3/2,z-1/2 #2 -x+1/2,-y+2,z-1/2

#3 -x+1/2,-y+2,z+1/2 #4 x,-y+3/2,z+1/2

Table S3. Selected bond lengths (Å) and angles (°) for **2**.

Cd(1)-N(1)	2.236(3)	N(1)#1-Cd(1)-O(2)#2	95.31(9)
Cd(1)-N(1)#1	2.236(3)	O(1)#2-Cd(1)-O(2)#2	54.02(9)
Cd(1)-O(1)#2	2.322(3)	O(1)#3-Cd(1)-O(2)#2	116.46(12)
Cd(1)-O(1)#3	2.322(3)	O(2)#3-Cd(1)-O(2)#2	88.13(11)
Cd(1)-O(2)#3	2.441(2)	N(2)#4-Cd(2)-N(2)	169.33(15)
Cd(1)-O(2)#2	2.441(2)	N(2)#4-Cd(2)-O(6)	95.34(7)
Cd(2)-N(2)#4	2.242(3)	N(2)-Cd(2)-O(6)	95.34(7)
Cd(2)-N(2)	2.242(3)	N(2)#4-Cd(2)-O(5')#4	91.00(10)
Cd(2)-O(6)	2.289(4)	N(2)-Cd(2)-O(5')#4	88.82(10)
Cd(2)-O(5')#4	2.348(3)	O(6)-Cd(2)-O(5')#4	90.99(7)
Cd(2)-O(5)#4	2.348(3)	N(2)#4-Cd(2)-O(5)#4	91.00(10)
Cd(2)-O(5)	2.348(3)	N(2)-Cd(2)-O(5)#4	88.82(10)
Cd(2)-O(7)	2.356(4)	O(6)-Cd(2)-O(5)#4	90.99(7)
N(1)-Cd(1)-N(1)#1	106.71(14)	N(2)#4-Cd(2)-O(5)	88.82(10)
N(1)-Cd(1)-O(1)#2	89.65(10)	N(2)-Cd(2)-O(5)	91.00(10)
N(1)#1-Cd(1)-O(1)#2	97.12(13)	O(6)-Cd(2)-O(5)	90.99(7)
N(1)-Cd(1)-O(1)#3	97.12(13)	O(5)#4-Cd(2)-O(5)	178.02(14)
N(1)#1-Cd(1)-O(1)#3	89.65(10)	N(2)#4-Cd(2)-O(7)	84.66(7)
O(1)#2-Cd(1)-O(1)#3	168.67(18)	N(2)-Cd(2)-O(7)	84.66(7)
N(1)-Cd(1)-O(2)#3	95.31(9)	O(6)-Cd(2)-O(7)	180.0

N(1)#1-Cd(1)-O(2)#3	139.92(9)	O(5')#4-Cd(2)-O(7)	89.01(7)
O(1)#2-Cd(1)-O(2)#3	116.46(12)	O(5)#4-Cd(2)-O(7)	89.01(7)
O(1)#3-Cd(1)-O(2)#3	54.02(9)	O(5)-Cd(2)-O(7)	89.01(7)
N(1)-Cd(1)-O(2)#2	139.92(9)		

Symmetry transformations used to generate equivalent atoms in 2:

#1 -x+1,y,-z+1/2 #2 -x+1/2,y-1/2,-z+1/2

#3 x+1/2,y-1/2,z #4 -x+1,y,-z-1/2 #5 x-1/2,y+1/2,z

Table S4. Phosphorescence lifetime of the materials.

Samples		λ_{ex} (nm)	λ_{em} (nm)	τ_1(ms)	A_1(%)	τ_2(ms)	A_2(%)	τ_3(ms)	A_3(%)	T_{av}(ms)
H_2L		365	505	22	11.538	81	44.802	230	43.660	139.2
1		365	485	71	2.590	110	0.161	270	97.249	264.6
1-EtOH		365	485	32	2.810	170	4.882	180	92.308	175.4
2		365	495	0.00984	16.944	0.0844	65.931	0.15	17.125	0.083
2-NH_3	**6 ppm**	365	495	1.7	76.697	13	8.709	65	14.594	11.92
	12 ppm	365	495	10	11.232	51	69.628	130	19.140	61.52
	18 ppm	365	495	18	10.400	49	67.258	160	22.342	70.58
	24 ppm	365	495	7.4	9.452	48	69.190	180	21.358	72.36
2-DMAc		365	465	0.00924	2.192	0.0856	26.857	0.580	70.951	0.4346
2-DMAc-NH_3·H_2O		365	465	0.02049	0.158	0.820	17.051	1.8	82.792	1.630

Table S5. Comparison of sensing parameters between Cd-MOF (**1**) and other Fe^{3+} probes.

Probe	Type of Luminescence	LOD	Dispersing solvent	Line range	R^2	Refs.
Cd-MOF(1)	**RTP.**	**1.63 μM**	**EtOH**	**0 ~ 183 μM**	**0.998**	**This work**
Eu-MOF	Phos.	45 μM	EtOH	0 ~ 250 μM	0.992	(**2**)
1-(pyren-1-yl)-N,N-bis-(pyridine-2-ylmethyl)methanamine	Fluo.	4.9 μM	MeOH	10 ~ 45 μM (Abs)		(**3**)
Mg-LMOF（MgAPDA）	Fluo.	1.98×10^{-8} M	DMF	0 ~ 120 μM	0.9946	(**4**)
Cd-MOF-1 Cd-MOF-2	Fluo.	2.4 μM 74 μM	DMF			(**5**)
CD CD/PVA	Fluo. RTP	0.125 μM 0.57 μM	 H_2O	0 − 1 mM 0.1 − 2 mM	0.993 0.988	(**6**)
Ni-MOF	Fluo.	15.44 mM	EtOH		0.9567	(**7**)
CQDs	Fluo.	7.488 μM	H_2O	0 ~ 100 μM	0.952	(**8**)
Eu-MOF-1	Phos.	5×10^{-4} M	H_2O			(**9**)
Eu-MOF-2	Phos.	26 μM	EtOH	0 ~ 220 μM	0.98	(**10**)
Tb-MOF-1	Phos.	1×10^{-5} M	EtOH			(**11**)
Tb-MOF-2	Phos.	1×10^{-6} M	DMF	0 − 0.3 mM	0.99	(**12**)
Al/Sc-PMCs	Phos.	91.2 μM	H_2O	0.375 ~ 1 mM	0.991	(**13**)

Table S6. Comparison of sensing parameters between Cd-MOF (**2**) and other NH_3 Sensors.

Substance	Type of sensor	Theoretical detection limit	Detection environment	Refs.
Cd-MOF(2)	**Phos. (Turn on)**	**0.4 mM**	**DMAc**	**This work**
		3 ppm	**Air**	
Fe-MOF	Fluo. (Discoloration)	105 ppb	Air	(**14**)
$Ag_{10}Cu_6$ Cluster	Phos. (Turn off)	21 μM	H_2O	(**15**)
		53 ppm	Air	
Eu_4L_4	Fluo. (Turn on)	55.82 ppt	film	(**16**)
Zn-MOF Mg-MOF	Fluo. (Discoloration) Fluo. (Turn on)	-	-	(**17**)
Pb-MOF	Fluo. (Turn off)	12 ppm	Air	(**18**)
Co(II/III)-MOF	Fluo. (Discoloration) Red → brown	1.38 ppm	Air	(**19**)
Cd-MOF	Fluo. (Discoloration) cyan→ yellow-green	-	Air	(**20**)
Zn complex	Fluo. (Discoloration) red → orange	-	Air	(**21**)
Tb-MOF	Fluo. (Turn off)	-	-	(**22**)
$Cu^{II}_2OHCu^{I}(TMBD)_2 \cdot 2H_2O$	Fluo. (Discoloration) green → blue	-	Air	(**23**)
Zn complex	Fluo. (Discoloration) reddish-brown → red	-	Air	(**24**)
Z3	Fluo. (Discoloration) blue → red	-	Air	(**25**)
Mg-MOF (SNNU-88)	Fluo. (Turn on)	turn-off (0.1-1.5 ppm) turn-on (3.0-100 ppm)	DMAc	(**26**)
Zr-MOF	Fluo. (Turn on)	6.5 ppb (384 nM)	H_2O	(**27**)
$\{[Cd_4(HIDCPy)_6] \cdot 4DMF \cdot 4C_2H_8N \cdot H_2O\}_n$	Fluo. (Turn on)	-	H_2O	(**28**)
$[Zn_3L_2(OAc)_4]1.5CH_3CN$	Fluo. (Discoloration) red → orange	-	Air	(**29**)
TPA power	Phos. (Discoloration) yellow → blue-green	-	Air	(**30**)

3. Figures

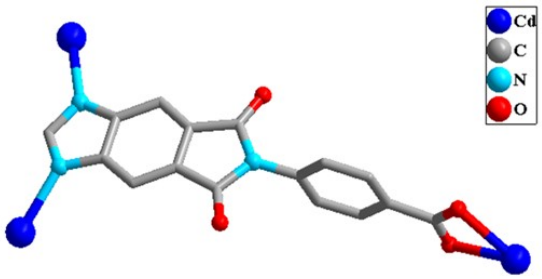

Figure S1. Coordination mode of the ligand in **1** and **2**.

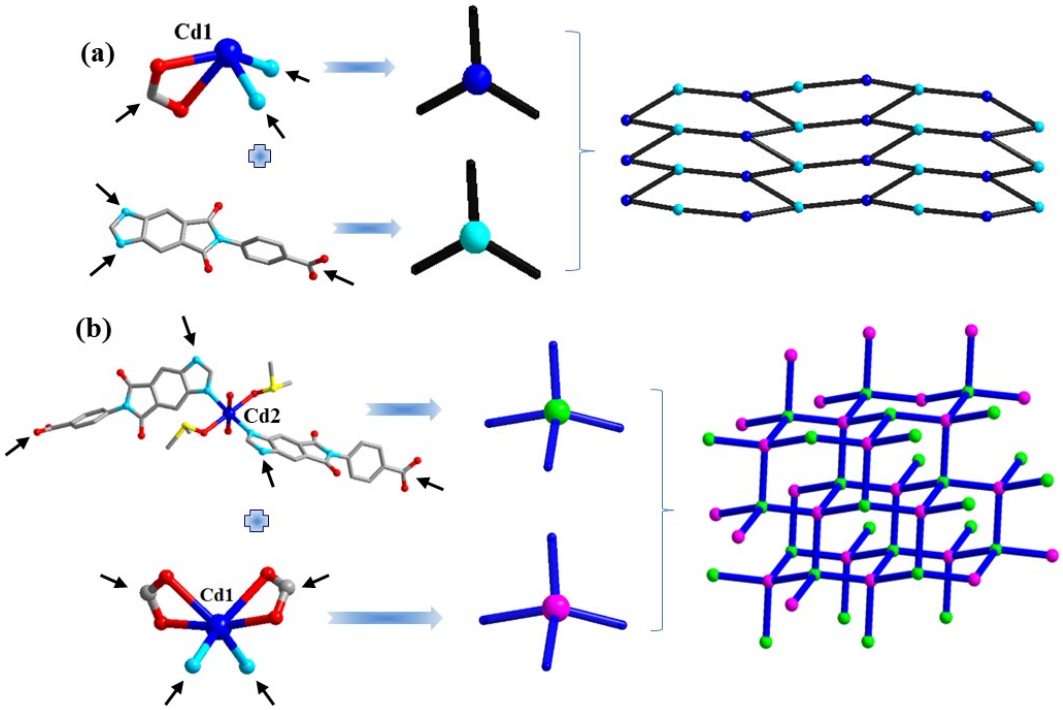

Figure S2. (a) Schematic representation of the (6, 3)-connected 2D honeycomb topological net of **1**. (b) Schematic representation of the (4, 4)-connected 3D dia topological net of **2**.

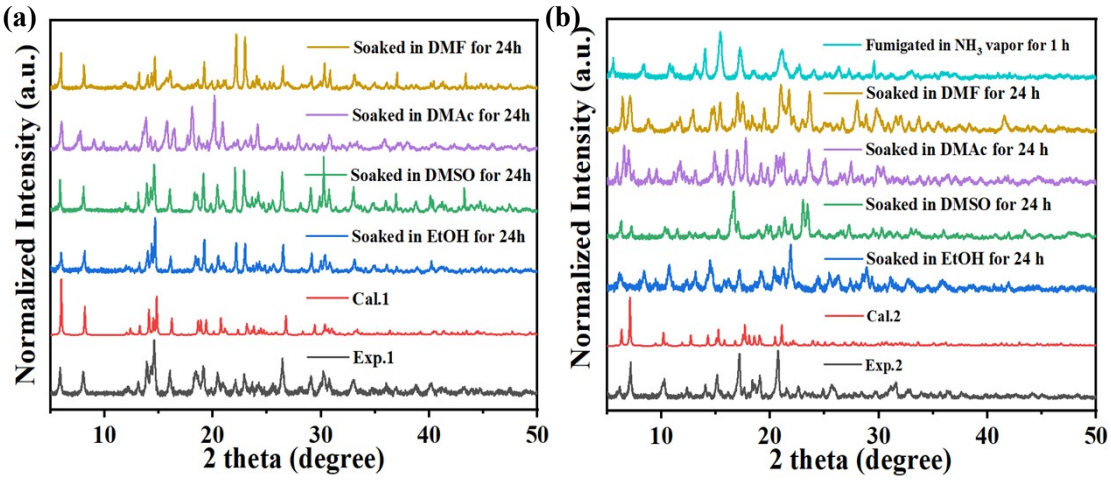

Figure S3. (a) A comparison of the calculated and experimental PXRD patterns of **1**, patterns of **1** after soaked in different solvents for 24 h. (b) A comparison of the calculated and experimental PXRD patterns of **2**, patterns of **2** after soaked in different solvents for 24 h and fumigated in NH_3 vapor for 1 h.

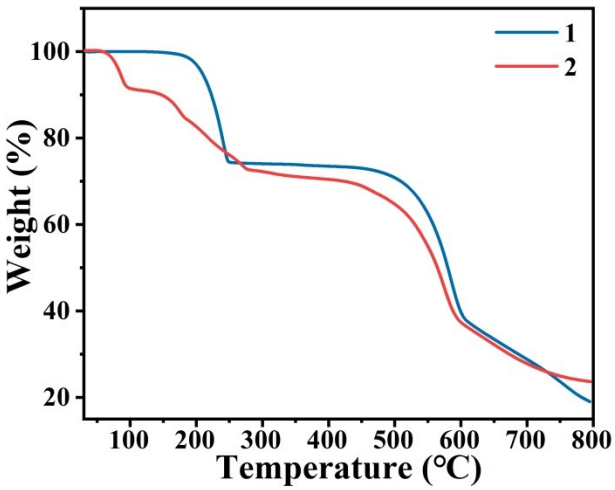

Figure S4. TGA curves of **1** and **2**.

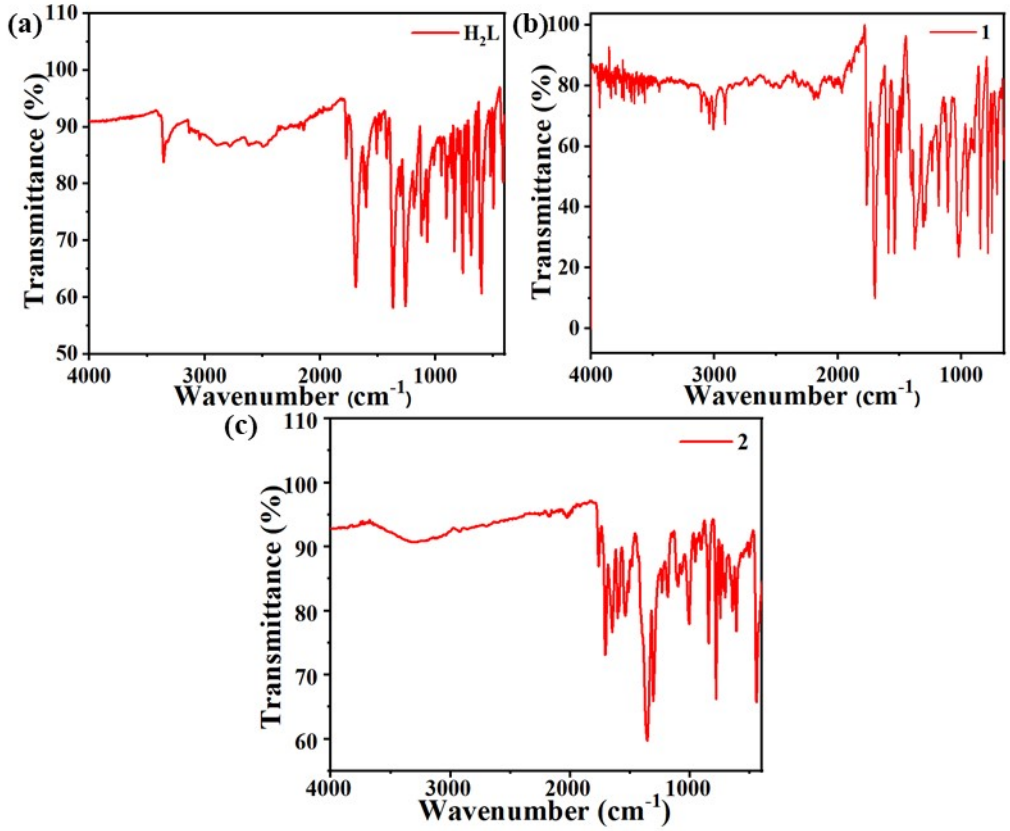

Figures S5. IR spectra of H_2L (a), **1** (b) and **2** (c).

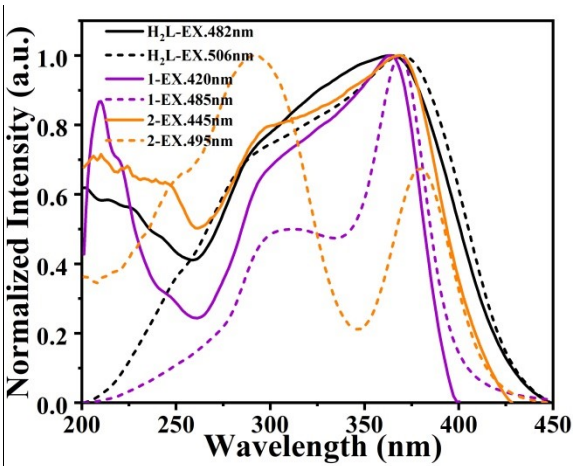

Figure S6. Excitation spectra of H_2L, **1** and **2**.

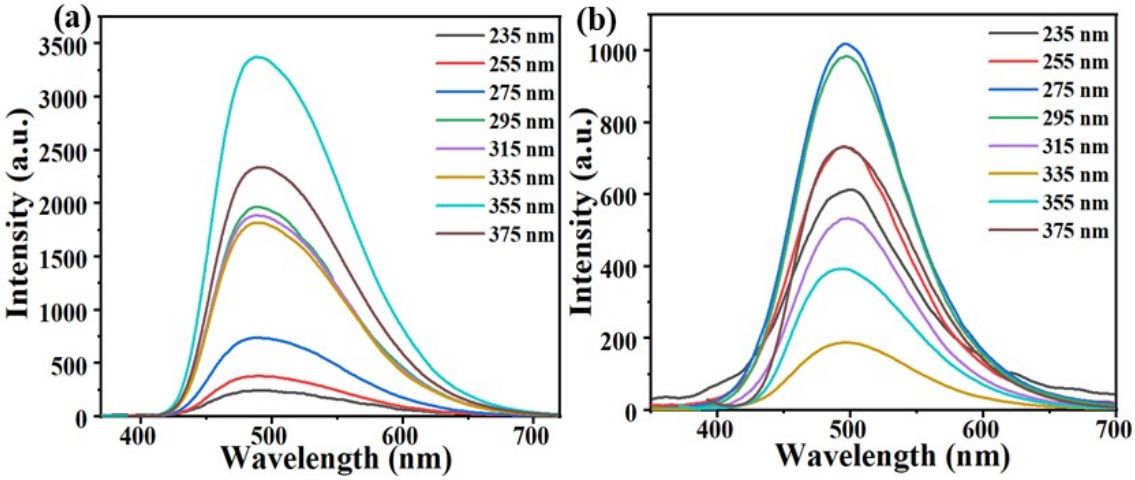

Figure S7. Delayed emission spectra of **1** (a) and **2** (b) at different excitation wavelengths.

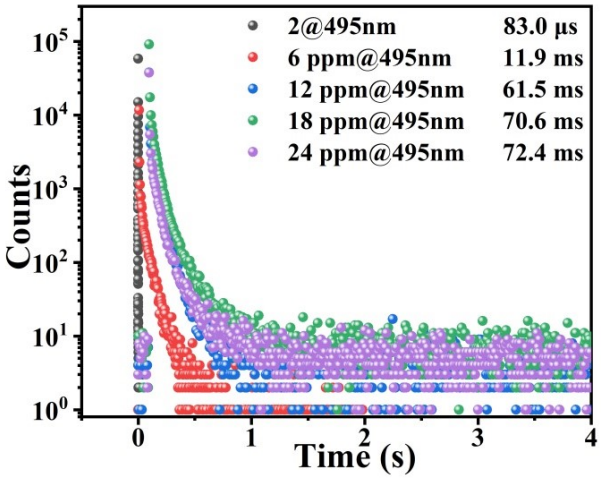

Figure S8. Time-resolved PL delay curves of **2** and **2**-NH_3 (the concentration of NH_3 vapor are 6, 12, 18 and 24 ppm respectively) at 495 nm. (λ_{ex} = 365 nm)

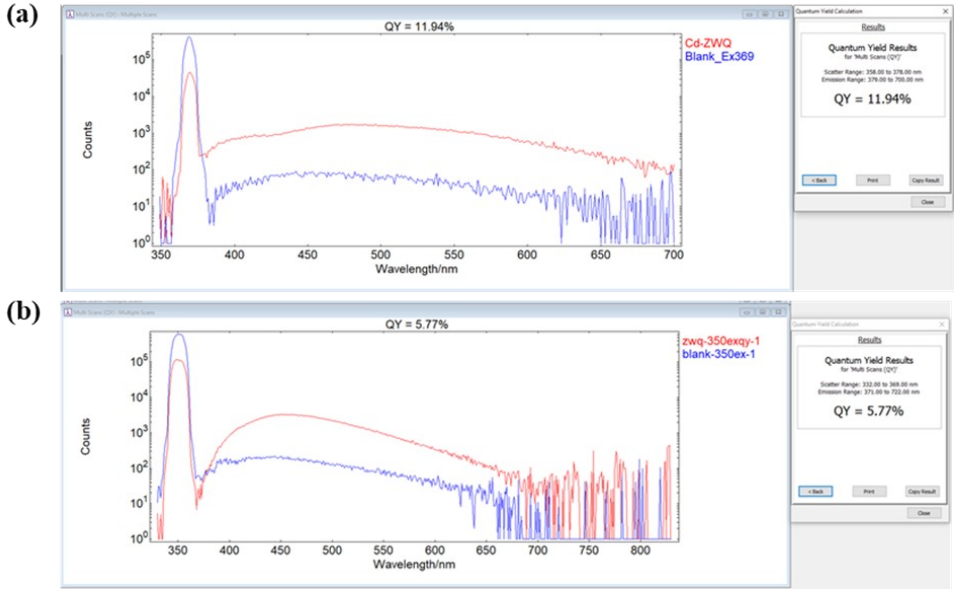

Figure S9. PL quantum yield of (a) **1** and (b) **2**.

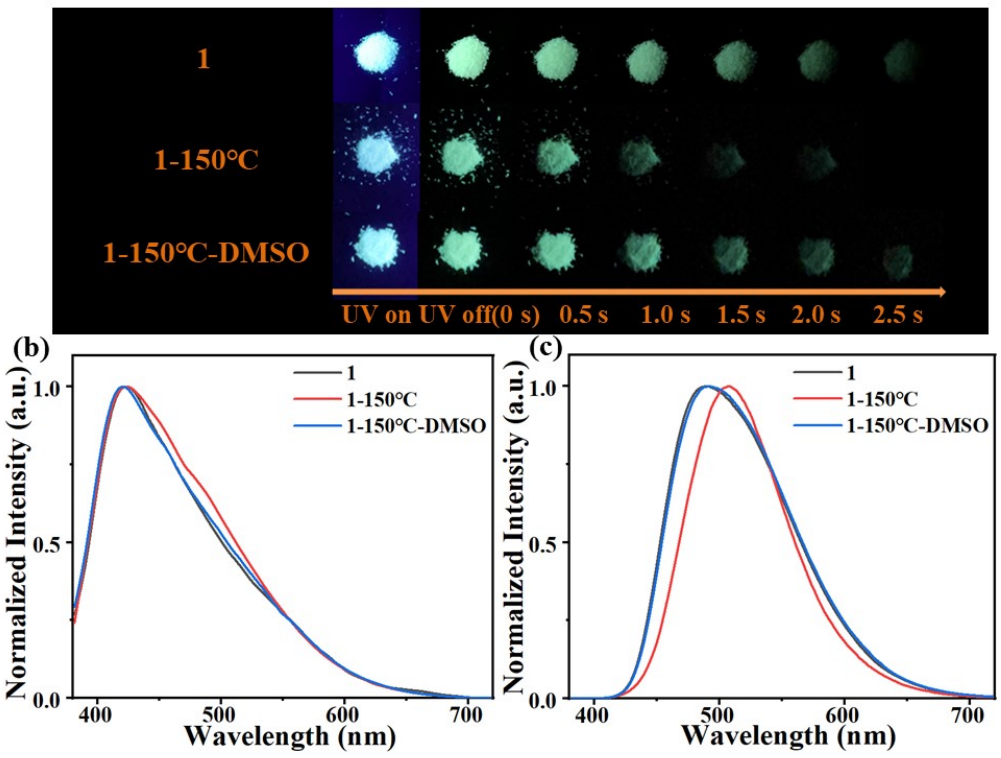

Figure S10. (a) Luminescence photos of **1**, **1** after heated at 150℃ for 15 mins (**1-150℃**), and then soaked in DMSO for ~ 8 hours (**1-150℃-DMSO**). Prompt (b) and delayed (c) PL emission spectra. (λ_{ex} = 365 nm)

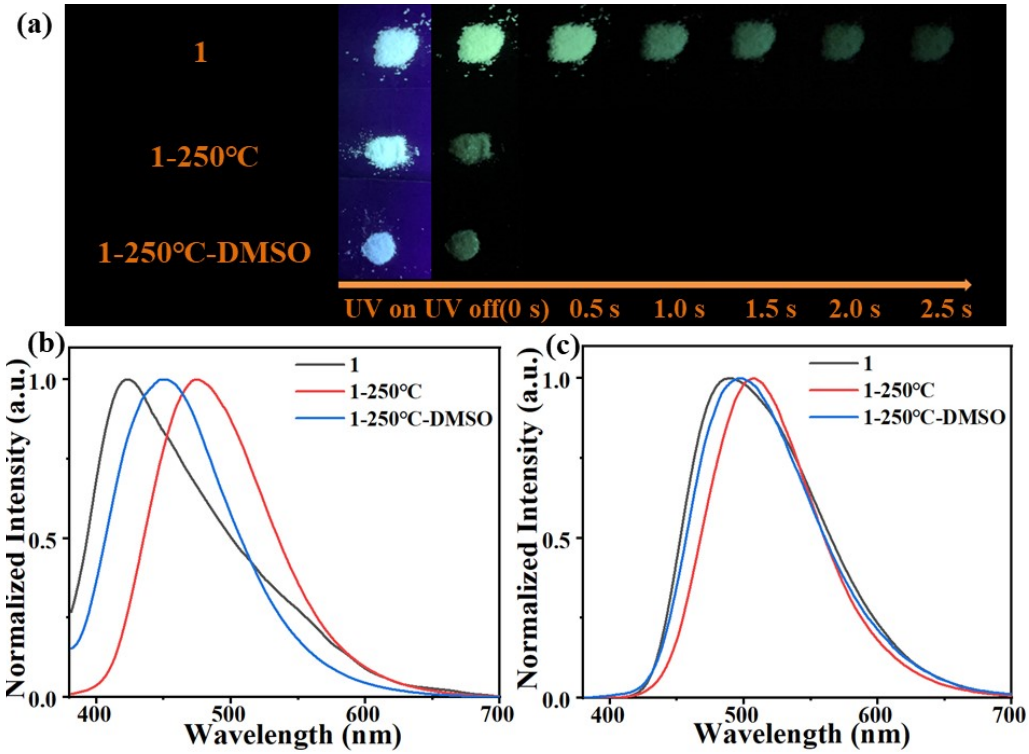

Figure S11. (a) Luminescence photos of **1** and **1** heated at 250°C for 15 mins (**1-250°C**) and then soaked in DMSO for ~ 15 hours (**1-250°C-DMSO**); Prompt (b) and delayed (c) PL emission spectra. (λ_{ex} = 365 nm).

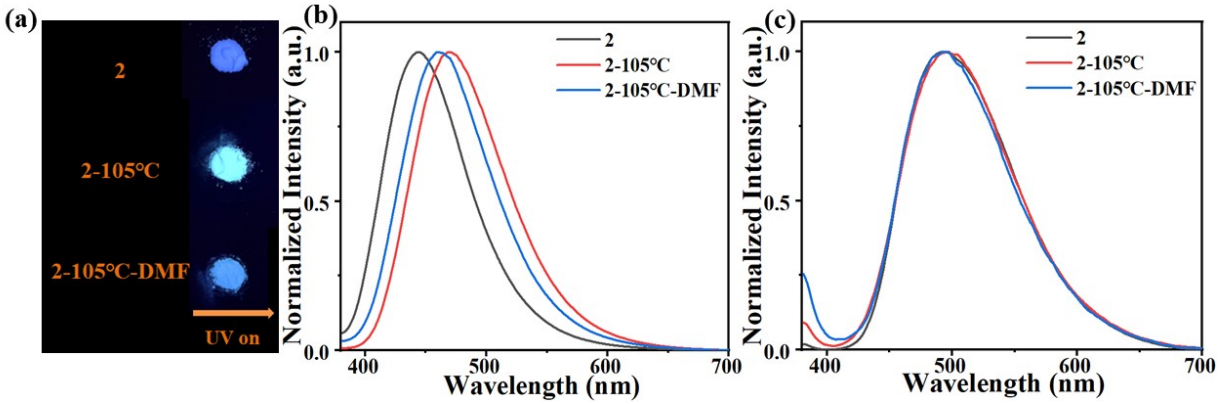

Figure S12. (a) Luminescence photos of **2** and **2** heated at 105°C for 15 mins (**2-105°C**) and then soaked in DMSO for ~ 4 hours (**2-105°C-DMF**); Prompt (b) and delayed (c) PL emission spectra. (λ_{ex} = 365 nm).

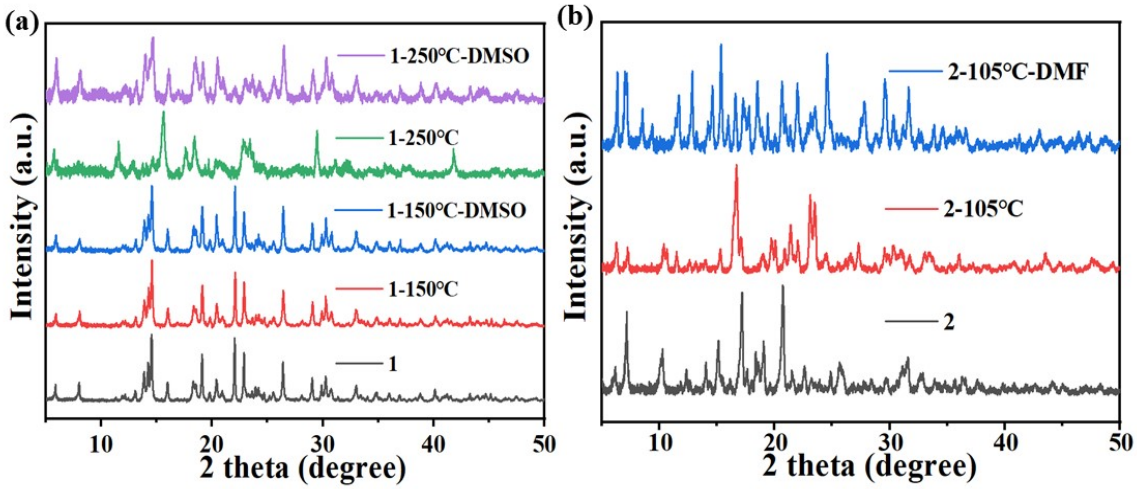

Figure S13. (a) PXRD patterns of **1** and **1** heated at 150°C and 250°C for 15 mins (**1-105°C/250°C**), then soaked in DMSO for ~ 8 hours/15 hours (**1-150°C/250°C-DMSO**). (b) PXRD spectra of **2** and **2** heated at 105°C for 15 minutes (**2-105°C**) and then soaked in DMF for ~ 4 hours (**2-105°C-DMF**).

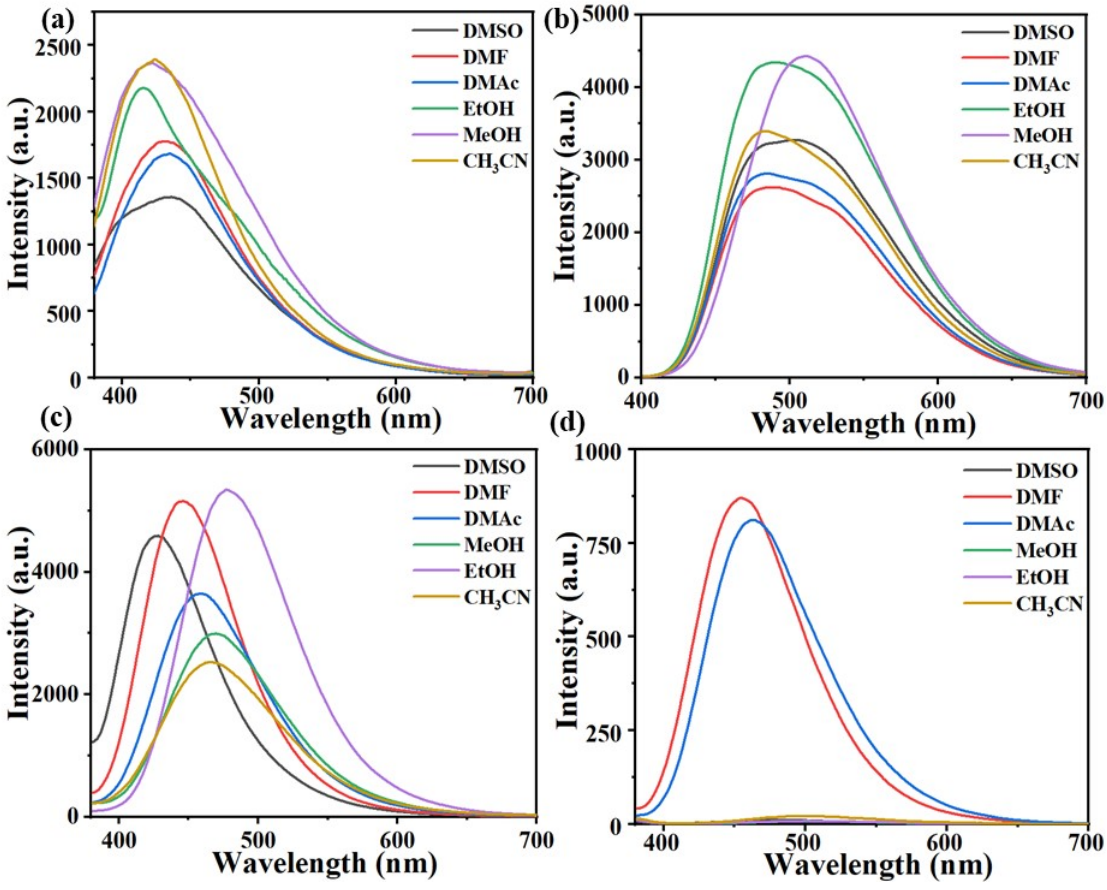

Figure S14. Prompt (a) and delayed (b) emission spectra of **1**' s suspensions of different solvents. Prompt (c) and delayed (d) emission spectra of **2**' s suspensions of different solvents. λ_{ex}= 365 nm. The excitation slit width and emission slit width were set to be 20 nm and 20 nm in the measurement of **2**'s delayed spectra.

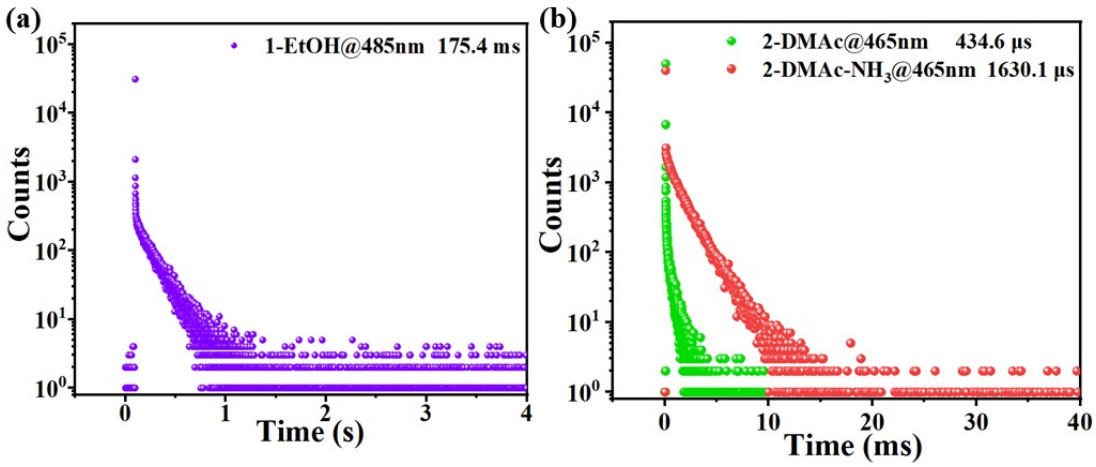

Figure S15. (a) Time-resolved PL decay curve of **1**' s EtOH suspension at 485 nm. (b) Time-resolved PL decay curve of **2**' s DMAc suspension before and after the addition of NH_3 (44.3 mM) at 465 nm.

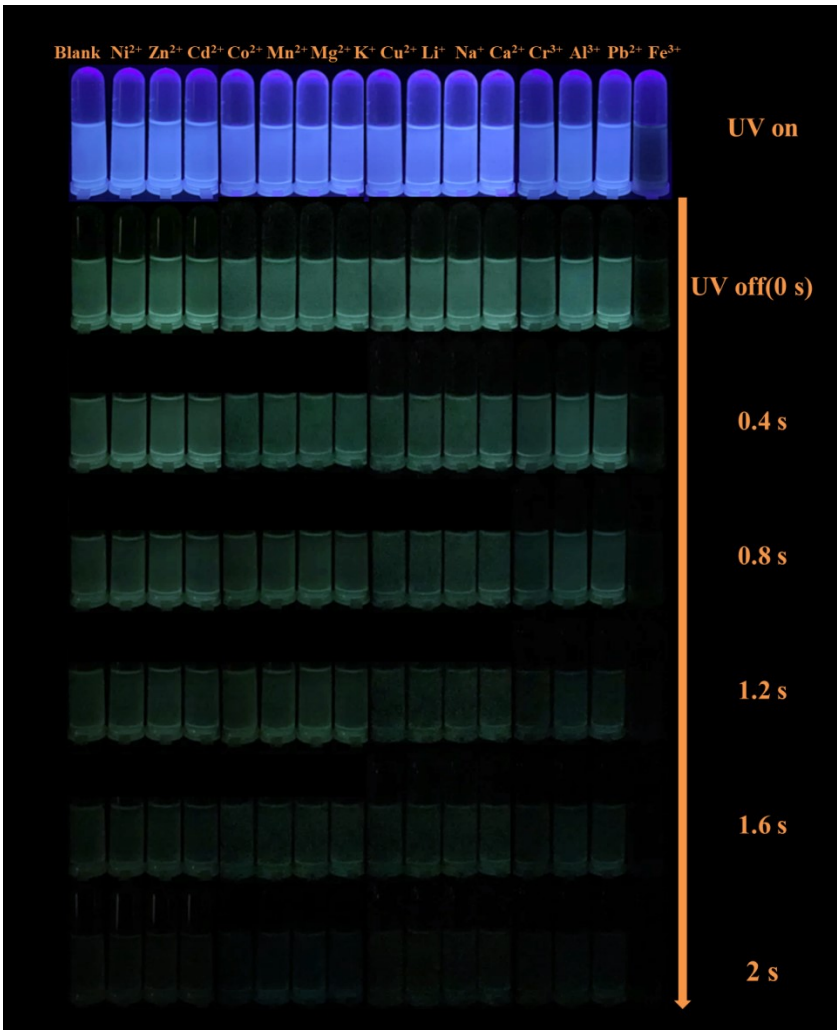

Figure S16. Luminescence photos of **1**'s EtOH suspensions in the presence of various metal cations (1 mM) under irradiation and upon removal of a 365 nm UV lamp.

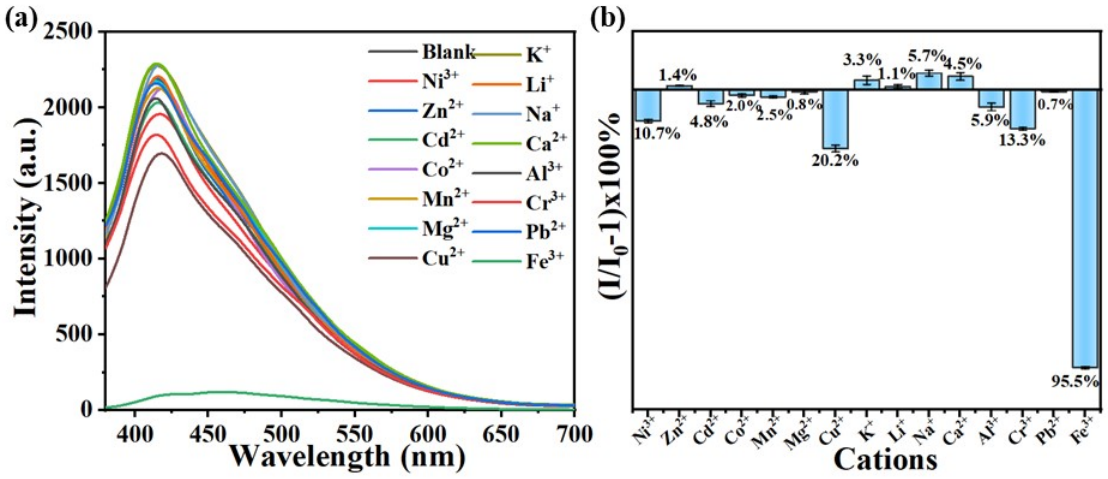

Figure S17. Prompt emission spectra (a) and the corresponding impacting efficiency of **1**'s suspensions in the presence of various metal cations (1 mM). λ_{ex} = 365 nm.

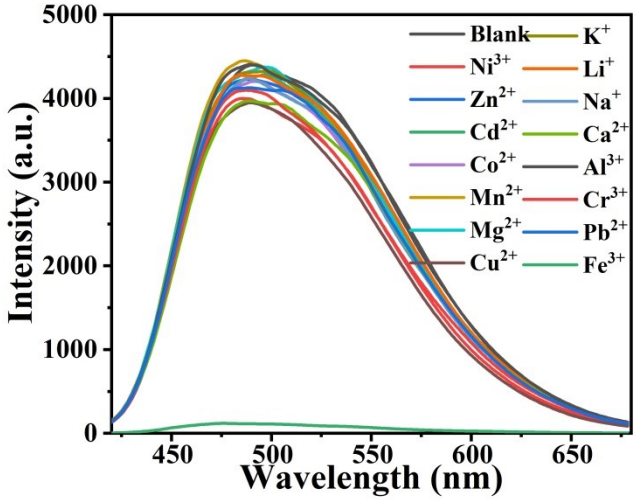

Figure S18. Delayed emission spectra of **1**'s EtOH suspensions in the presence of various metal ions (1 mM). λ_{ex}= 365 nm.

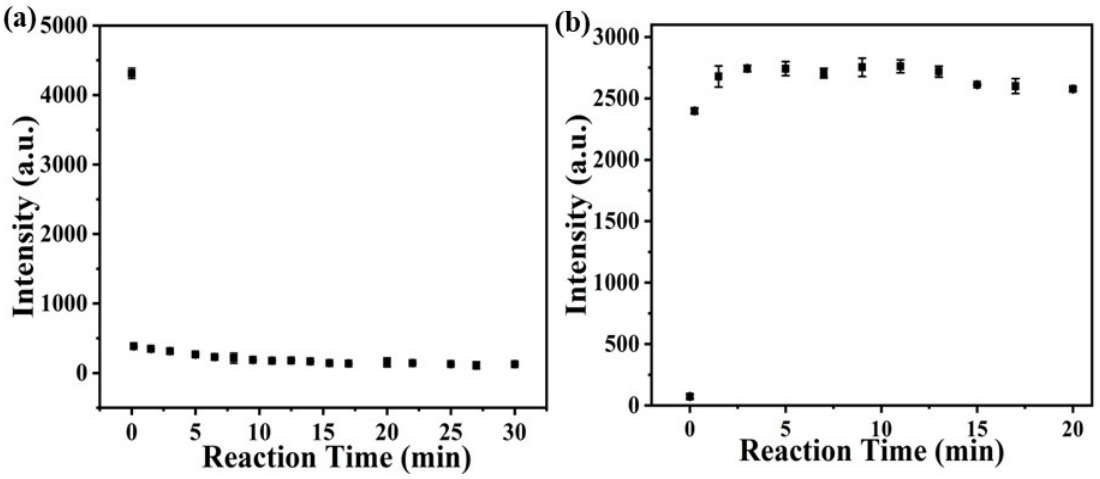

Figure S19. Luminescence intensity of the delayed emission of suspension of **1** (I_{485}) (a) and **2** (I_{465}) (b) as

a function of time when 1 mM Fe^{3+} solution or 44.3 mM $NH_3 \cdot H_2O$ were added, respectively. λ_{ex} = 365 nm

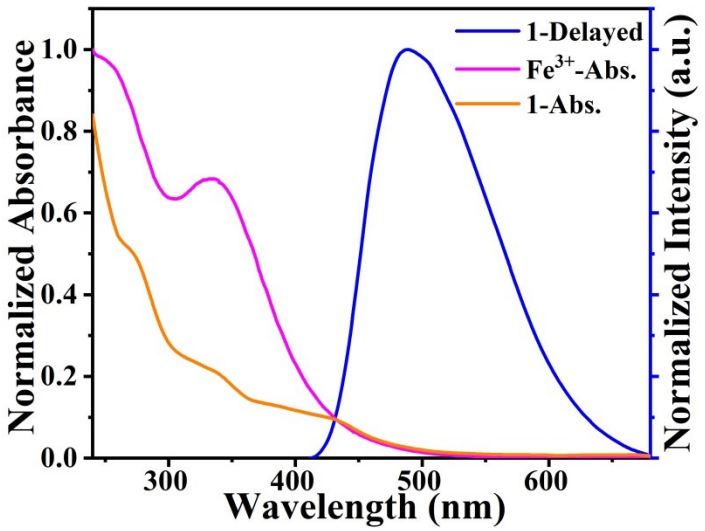

Figure S20. A comparison of delayed emission spectrum of **1**, UV-Vis absorption spectra of Fe^{3+} (1.0×10^{-4} M) and **1**'s EtOH suspension. λ_{ex} = 365 nm.

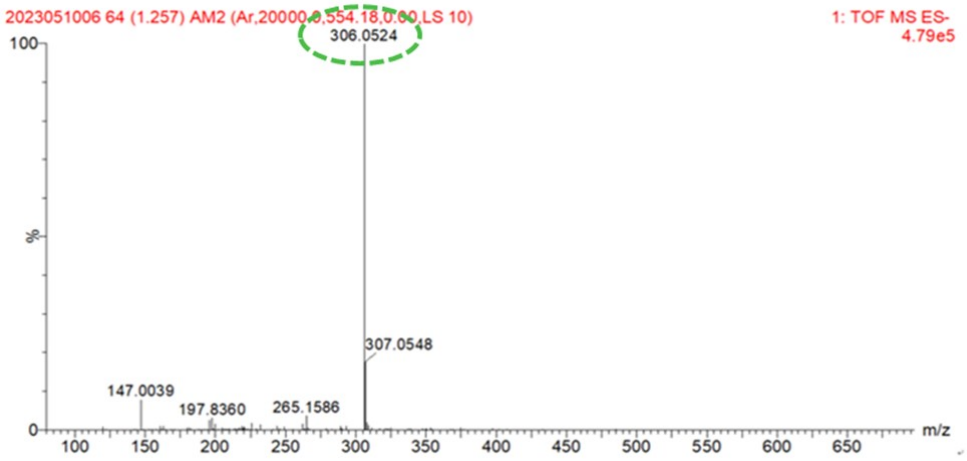

Figure S21. MS spectrum of **1**'s EtOH suspension after adding Fe^{3+}.

$[HL]^-$, obsd m/z: 306.05; calcd m/z: 306.26.

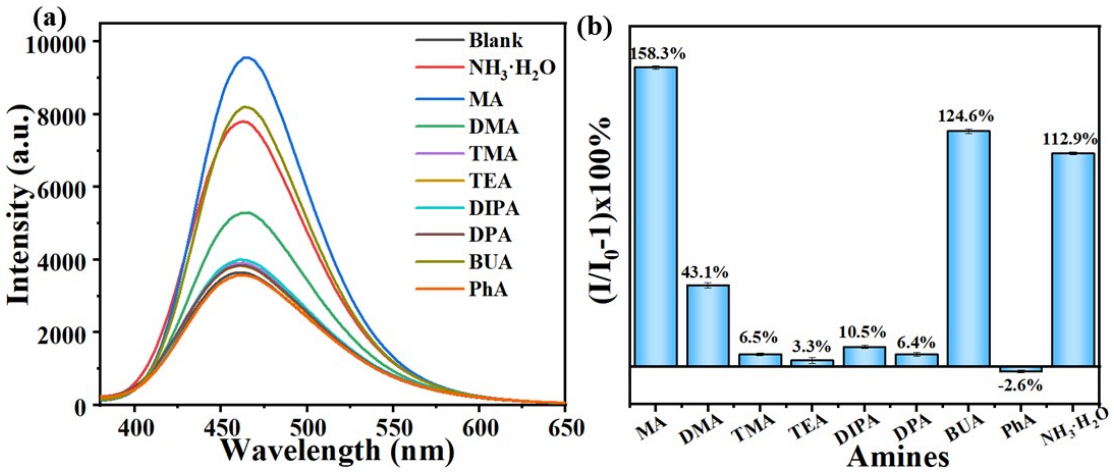

Figure S22. Prompt emission spectra (a) and the corresponding impacting efficiency (b) for **2**'s DMAc suspensions in the presence of various NH_3/amines (44.3 mM) (λ_{ex} = 365 nm).

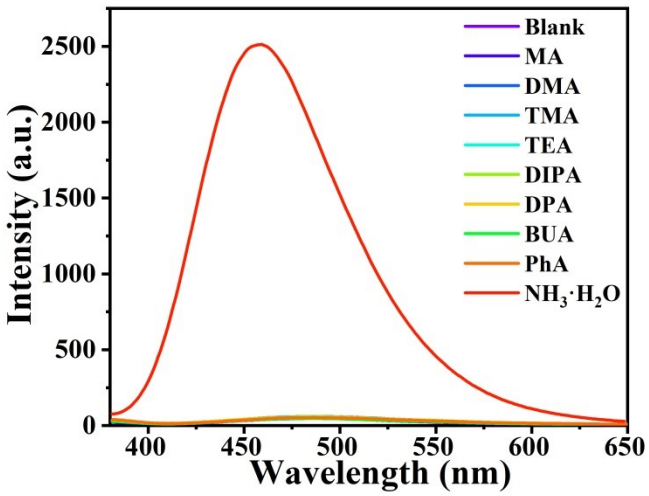

Figure S23. Delayed emission spectra of **2**'s DMAc suspensions in the presence of NH_3/amines (44.3 mM). λ_{ex} = 365 nm.

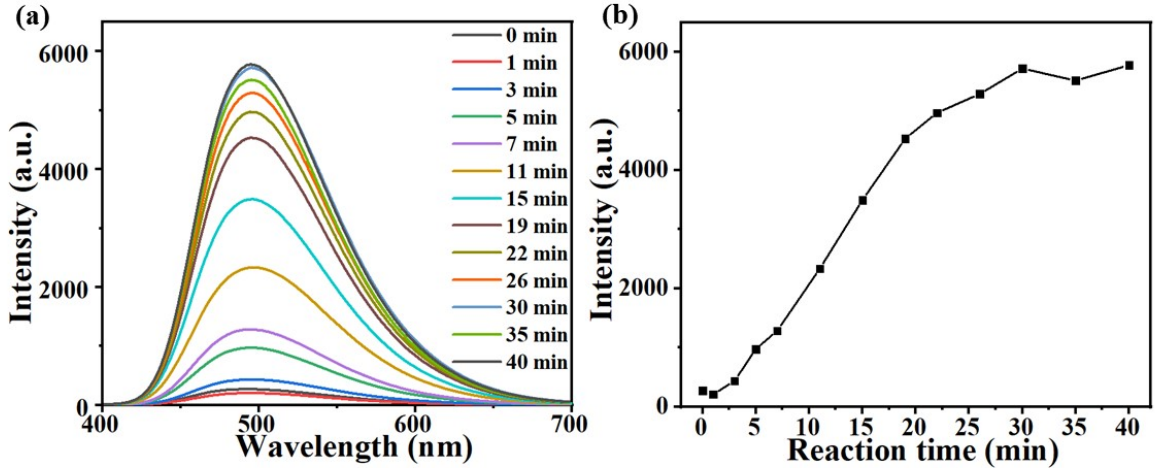

Figure S24. Time-dependent delayed spectra (a) of **2** in 25% NH_3 vapor and the corresponding kinetic curve (b). λ_{ex}= 365 nm.

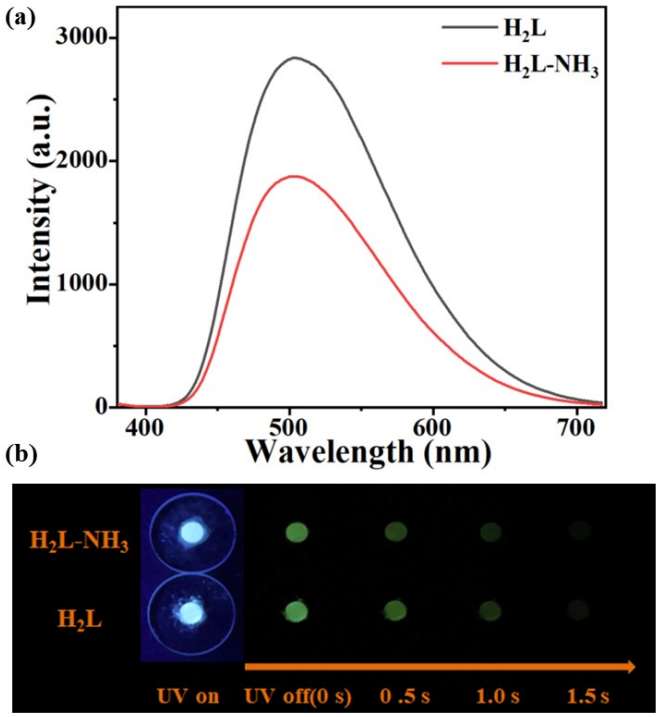

Figure S25. (a) Delayed emission spectra of H_2L before and after fumigated by NH_3 vapor. (b) The corresponding luminescence photos before and after turning off a 365 nm UV lamp.

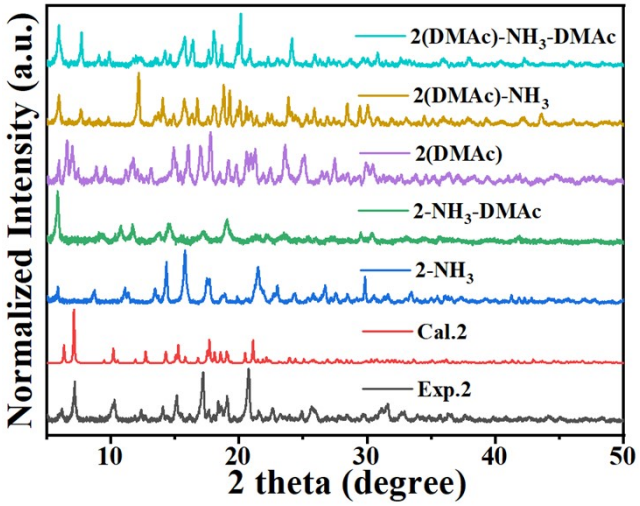

Figure S26. PXRD patterns of **2**, **2**(DMAc) (**2** soaked in DMAc), **2**(DMAc)-NH_3 (**2**(DMAc) treated with $NH_3{\cdot}H_2O$), **2**(DMAc)-NH_3-DMAc (**2**(DMAc)-NH_3 washed by DMAc), **2**-NH_3 (solid sample fumigated by NH_3 vapor), and **2**-NH_3-DMAc (**2**-NH_3 washed by DMAc).

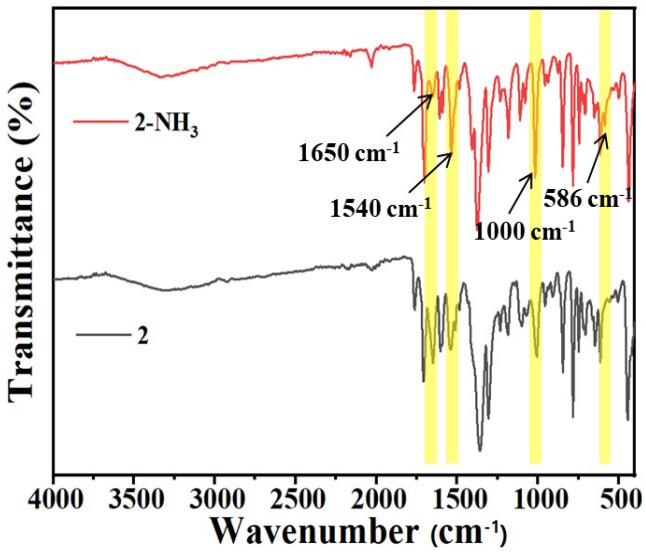

Figure 27. IR spectra of **2** and **2-NH$_3$** (solid sample fumigated by NH_3 vapor).

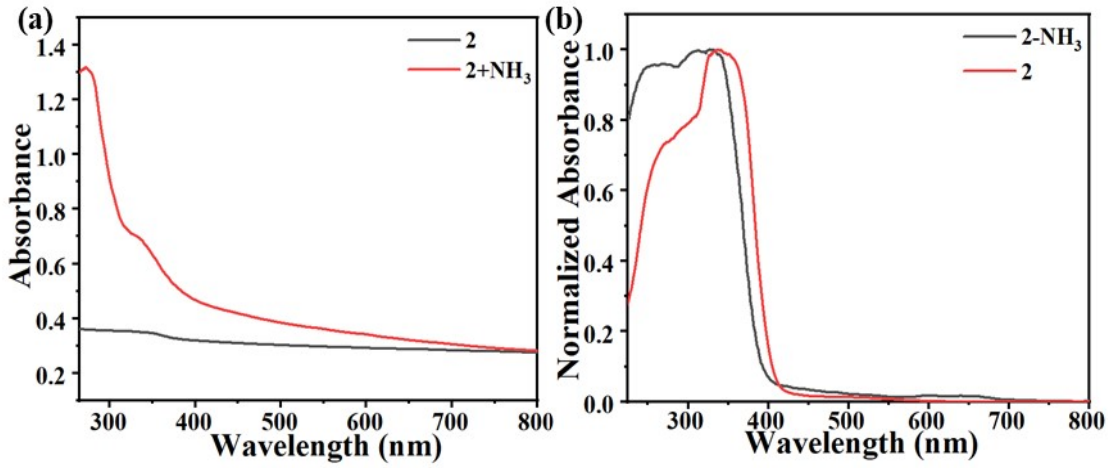

Figure S28. (a) UV-vis absorption spectra of **2**'s DMAc suspensions before and after adding 44.3 mM $NH_3 \cdot H_2O$. (b) Solid UV-vis absorption spectra of **2** before and after fumigated with NH_3 vapor.

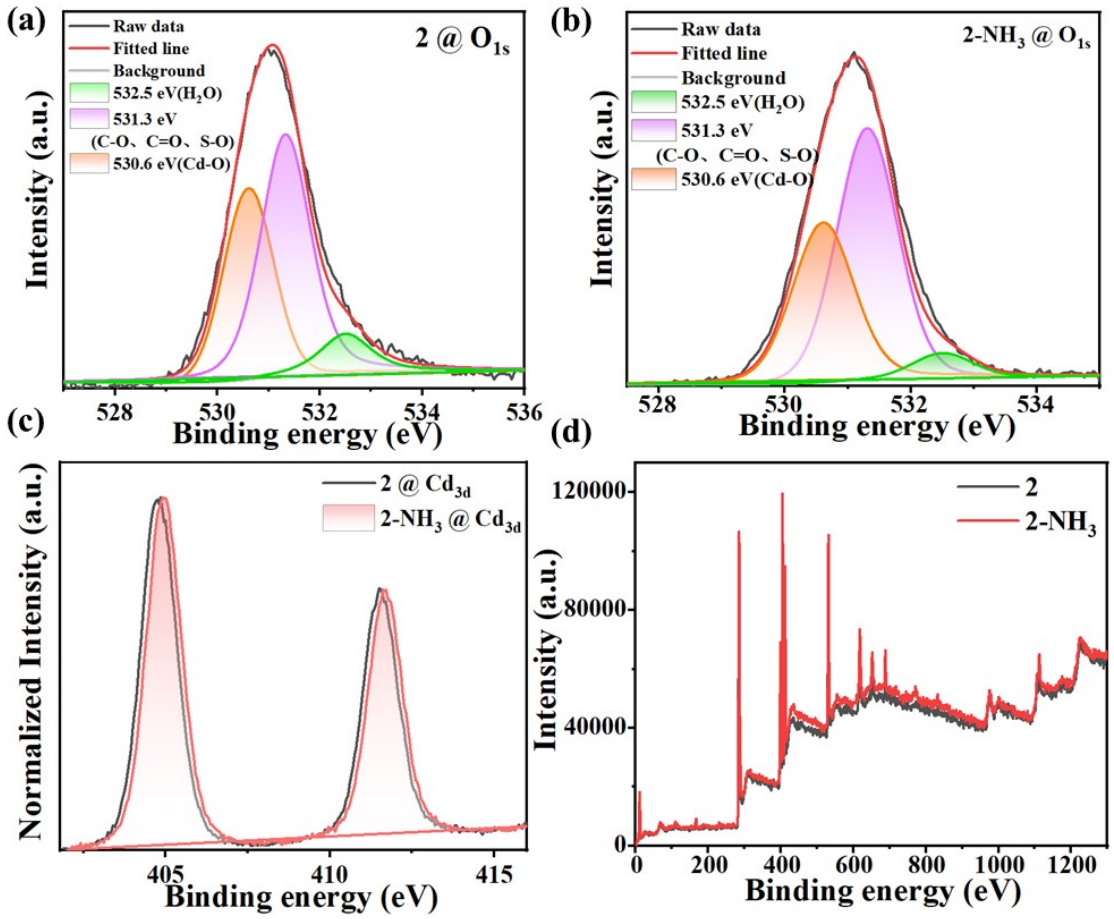

Figure S29. (a) 2@O_{1s}, (b) 2-NH_3@O_{1s}, (c) Cd_{3d} and (d) XPS spectra of **2** and **2** fumigated by NH_3 vapor (**2-NH_3**)

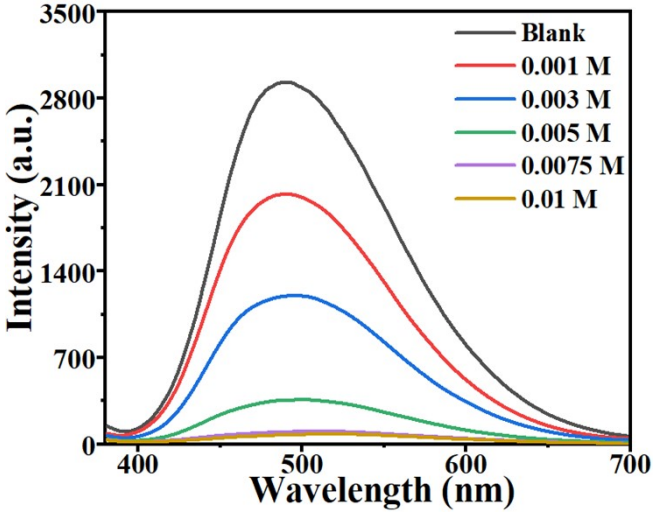

Figure S30. PL delayed spectra of test papers after dropping 30 μL different concentrations of Fe^{3+} solutions. (λ_{ex} = 365 nm**)**

REFERENCES

(1) J.-S. Yang, J. Zhu, R.-B. Liu, J. Ni, Z.-D. Chang, T. Hu, J.-J. Zhang and C.-G. Meng, *Inorg. Chim. Acta*, 2013, **394**, 117-126.

(2) Y. Kang, X.-J. Zheng and L.-P. Jin, *J. Colloid Interface Sci.*, 2016, **471**, 1-6.

(3) D. Phapale, A. Gaikwad and D. Das, *Spectrochim. Acta. A.*, 2017, **178**, 160-165.

(4) N. Xu, Q. Zhang, B. Hou, Q. Cheng and G. Zhang, *Inorg. Chem.*, 2018, **57**, 13330-13340.

(5) S. Chand, M. Mondal, S. C. Pal, A. Pal, S. Maji, D. Mandal and M. C. Das, *New J. Chem.*, 2018, **42**, 12865-12871.

(6) X. Wu, C. Ma, J. Liu, Y. Liu, S. Luo, M. Xu, P. Wu, W. Li and S. Liu, *ACS Sustainable Chem. Eng.*, 2019, **7**, 18801-18809.

(7) E. P. Asiwal, D. S. Shelar, C. S. Gujja, S. T. Manjare and S. D. Pawar, *New J. Chem.*, 2022, **46**, 12679-12685.

(8) H. Eskalen, S. Uruş, M. Kavgacı, H. V. Kalmı and B. Tahta, *Biomass Convers.*, 2023, DOI: 10.1007/s13399-023-04048-5.

(9) M. Zheng, H. Tan, Z. Xie, L. Zhang, X. Jing and Z. Sun, *ACS Appl. Mater. Interfaces*, 2013, **5**, 1078-1083.

(10) G.-P. Li, G. Liu, Y.-Z. Li, L. Hou, Y.-Y. Wang and Z. Zhu, *Inorg. Chem.*, 2016, **55**, 3952-3959.

(11) H. Xu, H.-C. Hu, C.-S. Cao, B. Zhao, *Inorg. Chem.*, 2015, **54**, 4585-4587.

(12) Q. Zhang, J. Wang, A. M. Kirillov, W. Dou, C. Xu, C. Xu, L. Yang, R. Fang and W. Liu, *ACS Appl. Mater. Interfaces*, 2018, **10**, 23976-23986.

(13) L. Y. Liang, B. B. Chen, Y. T. Gao, J. Lv, M. L. Liu and D. W. Li, *Adv. Mater.* 2023, 202308180.

(14) L. Sun, A. Rotaru and Y. Garcia, *J. Hazard. Mater.*, 2022, **437**, 129364.

(15) Y. Wang, J. J. Yan, S. Hu, D. James Young, H. X. Li and Z. G. Ren, *Chem. – An Asian J.*, 2021, **16**, 1-7.

(16) Y. Yao, Y. Zhou, T. Zhu, T. Gao, H. Li and P. Yan, *ACS Appl. Mater. Interfaces*, 2020, **12**, 15338-15347.

(17) N. B. Shustova, A. F. Cozzolino, S. Reineke, M. Baldo and M. Dincă, *J. Am. Chem. Soc.*, 2013, **135**, 13326-13329.

(18) X. Chen, Y. Yu, C. Yang, J. Yin, X. Song, J. Li and H. Fei, *ACS Appl. Mater. Interfaces*, 2021, **13**, 52765-52774.

(19) J. Zhang, J. Ouyang, Y. Ye, Z. Li, Q. Lin, T. Chen, Z. Zhang and S. Xiang, *ACS Appl. Mater. Interfaces*, 2018, **10**, 27465-27471.

(20) C. Wang, T. Zhang, L.-X. Sun, Y.-H. Xing and F.-Y. Bai, *Inorg. Chem. Front.*, 2023, **10**, 7351-7358.

(21) H.-W. Zheng, D.-D. Yang, Y.-S. Shi, T. Xiao and X.-J. Zheng, *Dalton Trans.*, 2022, **51**, 15370-15375.

(22) I. A. Ibarra, T. W. Hesterberg, J.-S. Chang, J. W. Yoon, B. J. Holliday and S. M. Humphrey, *Chem. Commun.*, 2013, **49**, 7156.

(23) X.-P. Zhou, Z. Xu, J. He, M. Zeller, A. D. Hunter, R. Clérac, C. Mathonière, S. S.-Y. Chui and C.-M. Che, *Inorg. Chem.*, 2010, **49**, 10191-10198.

(24) H.-W. Zheng, M. Wu, D.-D. Yang, Q.-F. Liang, J.-B. Li and X.-J. Zheng, *Inorg. Chem.*, 2021, **60**, 11609-11615.

(25) J. Ni, M.-Y. Li, Z. Liu, H. Zhao, J.-J. Zhang, S.-Q. Liu, J. Chen, C.-Y. Duan, L.-Y. Chen and X.-D. Song, *ACS Appl. Mater. Interfaces*, 2020, **12**, 12043-12053.

(26) Y.-P. Li, S.-N. Li, Y.-C. Jiang, M.-C. Hu and Q.-G. Zhai, *Chem.Commun.*, 2018, **54**, 9789-9792.

(27) D. I. Pavlov, T. S. Sukhikh, A. A. Ryadun, V. V. Matveevskaya, K. A. Kovalenko, E. Benassi, V. P. Fedin and A. S. Potapov, *J. Mater. Chem. C*, 2022, **10**, 5567-5575.

(28) J.-X. Ma, T. Zhou, T. Ma, Z. Yang, J.-H. Yang, Q. Guo, W. Liu, Q. Yang, W. Liu and T. Yang, *Cryst. Growth & Des.*, 2021, **21**, 383-395.

(29) H.-W. Zheng, D.-D. Yang, Q.-F. Liang and X.-J. Zheng, *New J. Chem.*, 2022, **46**, 4800 - 4805.

(30) Z. Cheng, H. Shi, H. Ma, L. Bian, Q. Wu, L. Gu, S. Cai, X. Wang, W.-W. Xiong, Z. An and W. Huang, *Angew. Chem. Int. Ed.*, 2018, **57**, 678-682.